

Increased Tumor Uptake of 3-¹²³I-Iodo-L- α -Methyltyrosine After Preloading with Amino Acids: An In Vivo Animal Imaging Study

Tony Lahoutte, MD; Vicky Caveliers, Pharm; Philippe R. Franken, MD, PhD; Axel Bossuyt, MD, PhD; John Mertens, PhD; and Hendrik Everaert, MD, PhD

Division of Nuclear Medicine, Academic Hospital, Free University Brussels, Brussels, Belgium

3-¹²³I-Iodo-L- α -methyltyrosine (3-IMT) is an amino acid analog used for tumor imaging. Specific accumulation is mediated mainly by the system L amino acid transport system. System L activity is known to increase when cells are loaded with amino acids. The aim of our study was to measure the effects of amino acid preload on ¹²³I-3-IMT tumor uptake and image contrast in a rat tumor model using in vivo dynamic imaging. **Methods:** Rhabdomyosarcoma (R1M) tumor-bearing rats underwent 2 dynamic ¹²³I-3-IMT studies on separate days: 1 baseline study and 1 after intraperitoneal injection (0.25 mmol/kg) of a single amino acid (arginine, proline, glutamate, asparagine, tryptophan, or phenylalanine) administered 30 min before intravenous injection of 18.5 MBq ¹²³I-3-IMT. A ^{99m}Tc-labeled human serum albumin study was performed on each rat for the calculation of the blood-pool activity inside the tumor. Time-activity curves were generated for tumor, contralateral background region, kidney, heart, and total body. Tumor uptake was corrected for blood-pool and background activity. Image contrast was calculated as the ratio between tumor and background activity. The rate (K_1) of tracer entering the tumor was obtained using Patlak analysis. A displacement study was performed on a separate group of rats, in which a high dose of phenylalanine was administered 40 min after ¹²³I-3-IMT injection. **Results:** ¹²³I-3-IMT accumulation in tumor reached a plateau 10 min after injection. Tumor uptake on the baseline scans correlated well with tumor size ($r = 0.92$). After preloading, tumor uptake and contrast increased in all conditions: arginine, +26% and +26%; proline, +15% and +13%; glutamate, +14% and +9%; asparagine, +19% and +15%; tryptophan, +36% and 11%; phenylalanine, +22% and +13%. K_1 values also increased. Administration of an afterload with phenylalanine induced a significant displacement of ¹²³I-3-IMT tumor accumulation. **Conclusion:** Prior amino acid administration increases ¹²³I-3-IMT tumor accumulation and image contrast. This effect can be explained by the increased antiporter activity of the amino acid transport system L in preloaded conditions. Our results indicate that the fasted state might not be the optimal metabolic condition to study tumor accumulation of L-transported tracers such as ¹²³I-3-IMT. Amino acid admin-

istration before ¹²³I-3-IMT injection could improve tumor uptake and image contrast.

Key Words: 3-¹²³I-Iodo-L- α -methyltyrosine; tumor imaging; system L; amino acid preload

J Nucl Med 2002; 43:1201-1206

Increased amino acid demand and transport across the cell membrane are an early feature of malignant transformation. The upregulated transport can be visualized using radiolabeled amino acid analogs. 3-¹²³I-Iodo-L- α -methyltyrosine (3-IMT) is a commonly used amino acid analog for SPECT and is applied for the clinical investigation of gliomas, head and neck squamous carcinomas, and several other types of extracerebral tumors (1-4). The accumulation of ¹²³I-3-IMT is fast and is mediated mainly by amino acid transport system L in most tissues (5-8). Once inside the cell, ¹²³I-3-IMT is not further metabolized. Several in vitro studies have shown that system L-type transporters are obligatory exchange mechanisms: They always exchange an intracellular amino acid for 1 or more extracellular amino acids (9,10). Therefore, system L activity is high when cells are loaded with amino acids and low when cells are depleted. Patient studies with ¹²³I-3-IMT are currently performed after several hours of fasting, a condition in which cells contain low levels of free amino acids. We hypothesized that prior administration (preload) of amino acids should positively influence ¹²³I-3-IMT accumulation. The aim of our study was to test this hypothesis by measuring the effects of preload with different amino acids on tumor accumulation of ¹²³I-3-IMT and on image contrast in a rat tumor model using an in vivo imaging protocol. In addition, we performed the reverse experiment by administering an amino acid load after ¹²³I-3-IMT injection, aimed at displacing accumulated ¹²³I-3-IMT in the tumor.

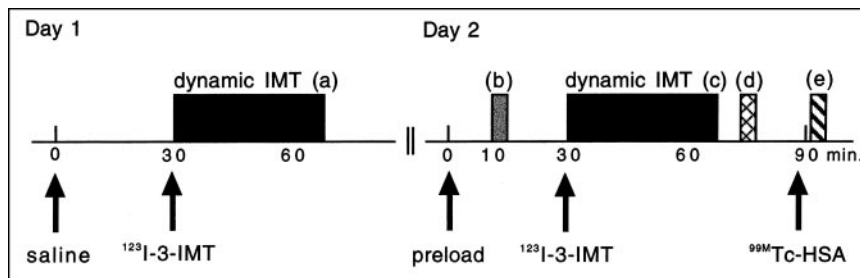
MATERIALS AND METHODS

¹²³I-3-IMT Tracer Synthesis

Radioiodination with ¹²³I (Nordion Europe, Fleurus, Belgium) of L- α -methyltyrosine (Sigma-Aldrich, St. Louis, MO) was per-

Received Sep. 24, 2001; revision accepted Jan. 22, 2002.
For correspondence contact: Tony Lahoutte, MD, Department of Nuclear Medicine, Academic Hospital, Free University Brussels (AZ VUB), Laarbeeklaan 101, B-1090 Jette, Belgium.
Email: tony.lahoutte@az.vub.ac.be

FIGURE 1. Scheme of imaging procedure: a, baseline dynamic ^{123}I -3-IMT acquisition; b, static acquisition of remaining ^{123}I activity of previous day; c, dynamic ^{123}I -3-IMT acquisition after preload; d, static acquisition for measurement of contribution of ^{123}I photons into $^{99\text{m}}\text{Tc}$ photopeak window; e, static $^{99\text{m}}\text{Tc}$ -HSA acquisition. Arrows indicate time of injection of indicated products.



formed by carrier-added electrophilic substitution using IODO-GEN (Pierce, Rockford, IL) as oxidizing agent. The reaction was performed at 0°C, and the reaction mixture was mixed for 2 min, yielding >90% ^{123}I -3-IMT (11). ^{123}I -3-IMT was separated in no-carrier-added concentrations using a small reverse-phase Sep-Pak column (Waters Millipore, Brussels, Belgium) as described by Gühlke and Biersack (12). A radiochemical purity of >99% was obtained.

Laboratory Animals

R1M rhabdomyosarcoma cells were obtained from Harlan (Horst, The Netherlands). Tumors were grown in the right flank of 2-mo-old male Wag/Rij rats ($n = 24$) after subcutaneous injection of $1 \cdot 10^6$ cells. Four weeks after injection, the tumors developed to volumes of 2–5 mL. At these volumes, the tumors were free of necrotic tissue. The animals had free access to water and food until 4 h before the imaging procedure. The animals were anesthetized using halothane during imaging. After the 2-d procedure, the animals were killed by intravenous injection of KCl. The study protocol was approved by the ethical committee for animal studies of our institution.

^{123}I -3-IMT Imaging

The time schedule of the imaging procedures is shown in Figure 1. Imaging was performed using a gamma camera equipped with medium-energy collimators. Dynamic ^{123}I -3-IMT (18.5 MBq intravenously) imaging was started 30 min after intraperitoneal injection of 5 mL 0.9% NaCl in baseline studies on day 1 and after intraperitoneal injection of 0.25 mmol/kg/5 mL 0.9% NaCl amino acid solution (arginine, proline, glutamate, asparagine, methionine, phenylalanine, or tryptophan) in preload studies on day 2. The chosen amino acids are typical substrates of different amino acid transport systems (Table 1). Control experiments were performed by repeating the baseline study on day 2 instead of a preload study. Two hundred forty images of 10 s each were acquired into 128 ×

128 matrices, using a 3.2 zoom factor (pixel size, 1.5 mm) and a photopeak window set at 15% around 159 keV (Fig. 1, a and c). Before the dynamic ^{123}I -3-IMT study on day 2, the remaining ^{123}I activity of the previous day was measured using a static acquisition of 5 min (Fig. 1, b). Dynamic ^{123}I -3-IMT images of day 2 were then corrected for the remaining ^{123}I activity of day 1.

$^{99\text{m}}\text{Tc}$ -HSA Imaging

$^{99\text{m}}\text{Tc}$ -Labeled human serum albumin (HSA) studies were performed to measure the relative blood-pool distribution to correct the ^{123}I -3-IMT tumor uptake for blood-pool activity. After the dynamic ^{123}I -3-IMT study on day 2, a static acquisition of 5 min (Fig. 1, d) was performed for the measurement of the contribution of ^{123}I photons into the $^{99\text{m}}\text{Tc}$ photopeak window (10% around 140 keV). Subsequently, the animals were injected intravenously with 74 MBq $^{99\text{m}}\text{Tc}$ -HSA (Mallinckrodt, Inc. B.V., Petten, Holland), and a static image of 5 min was acquired 10 min after injection (Fig. 1, e). The $^{99\text{m}}\text{Tc}$ -HSA image was then corrected for the contribution of ^{123}I photons.

Data Processing

Regions of interest (ROIs) were drawn around the tumor (T), the heart (H), the right kidney (R), and the total body (TB). A background ROI (BKG) of the same size as the T ROI was copied to the contralateral side. The injected dose (ID) was defined as the total count number inside the TB. Tracer uptake was expressed as the percentage ID (%ID). The counts inside the T and BKG of the ^{123}I -3-IMT studies were first corrected for blood-pool activity using the $^{99\text{m}}\text{Tc}$ -HSA study: The ratio (ρ_{tumor}) of counts inside the T versus the counts inside the H on the $^{99\text{m}}\text{Tc}$ -HSA image represents the amount of blood in the tumor relative to the amount of blood in the heart. Using this factor, we calculated the contribution of ^{123}I -3-IMT blood-pool activity to inside the T (T^{bp}) by multi-

TABLE 1
Ratio of Tumor Uptake, Tumor Contrast, and K_1 (Preload/Baseline)

| | $T^{\text{bp}, \text{BKG}}$ | | T/BKG | | K_1 | |
|---------------------------------|-----------------------------|-----------|-------|-----------|-------|-----------|
| | Ratio | Range | Ratio | Range | Ratio | Range |
| Control | 1.05 | 1.00–1.10 | 1.03 | 1.00–1.07 | 1.03 | 0.98–1.08 |
| Arginine (y ⁺ L) | 1.26 | 1.15–1.34 | 1.26 | 1.13–1.34 | 1.22 | 1.09–1.33 |
| Proline (ASC) | 1.15 | 1.05–1.22 | 1.13 | 1.06–1.24 | 1.13 | 1.01–1.30 |
| Glutamate (X_{AG}^-) | 1.14 | 1.03–1.20 | 1.09 | 1.02–1.15 | 1.04 | 0.94–1.15 |
| Asparagine (N) | 1.19 | 1.07–1.25 | 1.15 | 1.09–1.22 | 1.12 | 1.01–1.27 |
| Tryptophan (L) | 1.36 | 1.27–1.48 | 1.11 | 1.04–1.16 | 1.43 | 1.36–1.52 |
| Phenylalanine (L) | 1.22 | 1.22–1.23 | 1.13 | 1.02–1.23 | 1.06 | 0.97–1.15 |

$T^{\text{bp}, \text{BKG}}$ = tumor uptake corrected for blood-pool and background activity; T/BKG = tumor contrast; K_1 = rate of tracer entering tumor. Amino acids are typical substrates of listed amino acid transport system in parentheses.

plying ρ_{tumor} with the counts inside the H on the ^{123}I -3-IMT images for each image (the asterisks used throughout indicate corrected values). The blood-pool-corrected ^{123}I -3-IMT tumor uptake in function of time is then calculated as follows:

$$T^{*\text{bp}}(t) = T(t) - \rho_{\text{tumor}} \times H(t). \quad \text{Eq. 1}$$

The blood-pool-corrected counts inside the BKG ROI and R ROI was calculated using the same method. Second, the tumor uptake was corrected for background activity:

$$T^{*\text{bp},*\text{BKG}}(t) = T^{*\text{bp}}(t) - \text{BKG}^{*\text{bp}}(t). \quad \text{Eq. 2}$$

Tumor Uptake and Contrast

The ratio between the area under the curve (AUC) of the time-activity ($T^{*\text{bp},*\text{BKG}}(t)$) curves (AUC preload/AUC baseline) between 10 and 40 min after injection (plateau phase) was calculated for the comparison of tumor uptake in preloaded versus baseline conditions. Tumor contrast is defined as tumor-to-background ratio of the uncorrected data ($T(t)/\text{BKG}(t)$). For the comparison of tumor contrast in preloaded versus baseline conditions we calculated the ratio between the AUC of the $T(t)/\text{BKG}(t)$ curve (AUC preload/AUC baseline) between 10 and 40 min after injection. The number of pixels inside the tumor ROI was used as a measure of tumor size.

Patlak Analysis

A Patlak analysis of the data from the first 7 min was performed for the calculation of K_1 values (rate of tracer entering the tumor) using the following equation:

$$\frac{T(t)}{H(t)} = K_1 \frac{\int_0^t H(t) \cdot dt}{H(t)}. \quad \text{Eq. 3}$$

The graph of this equation gives a straight line with a slope equal to K_1 (13,14). The ratio of the K_1 values (preload/baseline) was calculated.

Displacement Study

Additional dynamic ^{123}I -3-IMT studies were performed in a separate group of tumor rats. A dynamic ^{123}I -3-IMT study (without preload) was performed for 60 min and at 40 min. After the injection of ^{123}I -3-IMT, 0.5 mL of 0.12 mol/L phenylalanine was administered intravenously. The time-activity curves were used to describe the effects.

Statistical Analysis

The parameters from the preload study were always compared with those from the baseline study of the same rat, thereby using each rat as its own control. Individual experiments were repeated 3 times. The results are expressed as the average ratio (preload/baseline) together with the range or SD when appropriate.

RESULTS

Baseline Study

The time-activity curves ($T(t)$, $K(t)$, $H(t)$, and $\text{BKG}(t)$) of a baseline ^{123}I -3-IMT study are shown in Figure 2. ^{123}I -3-IMT tumor activity reaches a plateau at 10 min after injection. Renal uptake is initially high and declines with time. The blood-pool activity declines rapidly after injection and becomes nearly constant afterward. Background activity is initially low but increases slowly with time.

The average tumor uptake ($T^{*\text{bp},*\text{BKG}}$), corrected for blood-pool and background activity, during the plateau phase (10–40 min after injection) of the baseline scans ranged between 3.3 and 22.9 %ID and correlated well ($r = 0.921$) with tumor size (Fig. 3). The activity measured inside the tumor ROI (T) can be subdivided into actual tumor uptake ($T^{*\text{bp},*\text{BKG}}$, $71\% \pm 8\%$), background activity

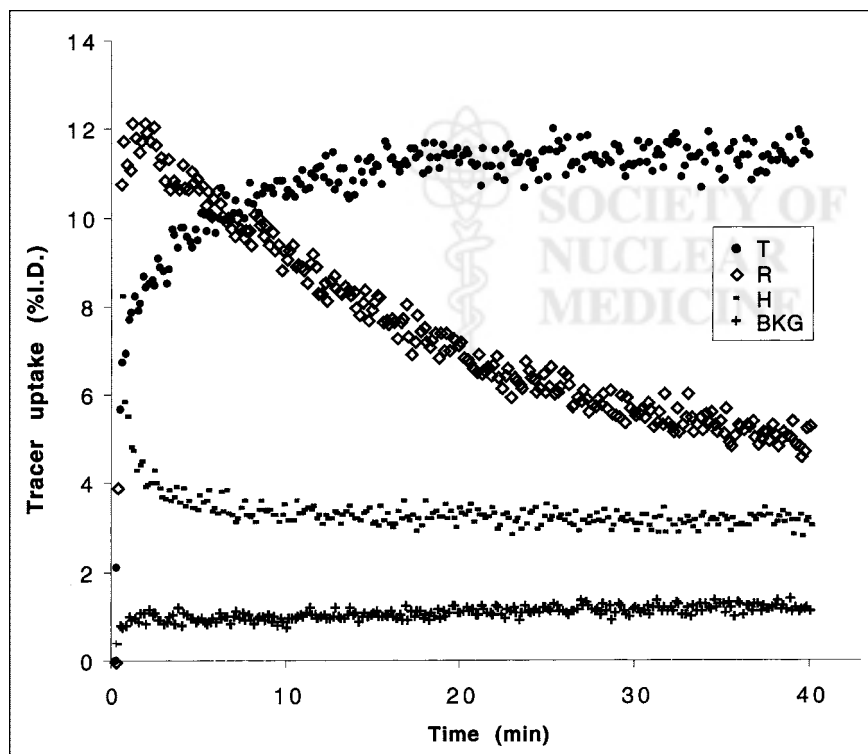


FIGURE 2. Time-activity curves representing tracer uptake (%ID) in tumor (T), right kidney (R), left ventricle (H), and contralateral background (BKG) region of ^{123}I -3-IMT baseline study in function time.

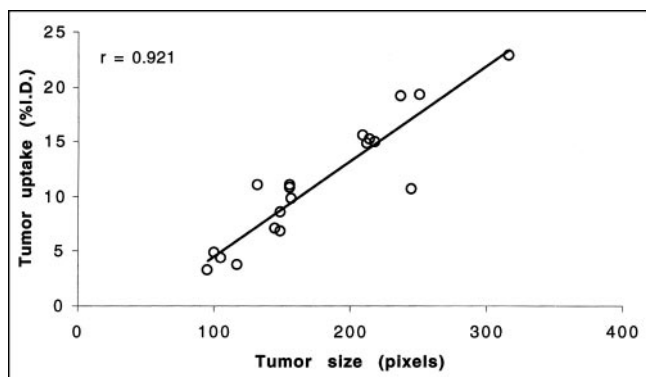


FIGURE 3. Correlation between tumor size and tumor uptake of baseline scans.

(BKG^{*bp}, 16% ± 5%), and blood-pool activity (*bp, 13% ± 5%). The tumor-to-background ratio averaged 5.4 ± 2.1.

Preload Study

Control studies, in which we repeated the baseline scan on day 2, showed good reproducibility of the methodology (Table 1). Visual analysis of the summed dynamic ¹²³I-3-IMT images showed improved image contrast after amino acid preload, especially in the case of arginine (Fig. 4). Increased tumor uptake (T^{*bp,*BKG}), tumor contrast (T/BKG), and rate of tracer entering the tumor (K_i) were measured after amino acid preload in all conditions (Table 1). The highest increase in tumor uptake was found after tryptophan (+36%), arginine (+26%), and phenylalanine (+22%) preload. The increase in tumor contrast was lower due to an increase in background activity, except for arginine (+26%). Patlak analysis of the initial uptake phase shows higher K_i values after amino acid preload in most cases. The most significant increase was measured after tryptophan preload.

Displacement Study

Tumor uptake decreased rapidly after intravenous administration of phenylalanine and reached a new plateau within minutes (Fig. 5). The activity released by the tumor was quickly captured by the kidneys.

DISCUSSION

As hypothesized, we measured an increased rate of tracer entering the tumor, higher tumor uptake, and improved image contrast after preload with several amino acids. Tryptophan, phenylalanine, and arginine induced the highest increase in ¹²³I-3-IMT tumor uptake. The increase in tumor uptake was matched by a similar increase in tumor contrast for arginine preload, whereas the improvement of tumor contrast was smaller for the other amino acids because of increased background activity. Administration of phenylalanine after ¹²³I-3-IMT injection induced an important displacement of ¹²³I-3-IMT tumor activity. The results can be explained by the characteristics of the transport processes responsible for ¹²³I-3-IMT transport.

Amino acid uptake across cellular membranes is mediated by different amino acid transport systems with overlapping substrate specificities (15). The most common transport systems include systems A, ASC, L, N, and X_{AG}⁻. Each of these systems accumulates only a selected group of amino acids with high affinity. Several in vitro studies have shown that ¹²³I-3-IMT accumulation is mediated mainly by system L (5–8). This system L transport activity is not performed by a single type of transporter protein but by a family of transporter proteins (LAT1, LAT2, y⁺LAT1, and so forth) with similar structure and function. The most common subtype is LAT1 and is used for the transport of neutral amino acids. An extensive review of this transporter family was recently published by Verrey et al. (9). A distinct characteristic of L-type transporters is that they are exchange mechanisms, exchanging intracellular amino acids for extracellular amino acids. Under physiologic conditions these transporters are believed to function in parallel with unidirectional transporters such as systems A and ASC (Fig. 6). The unidirectional systems use the Na⁺ gradient as

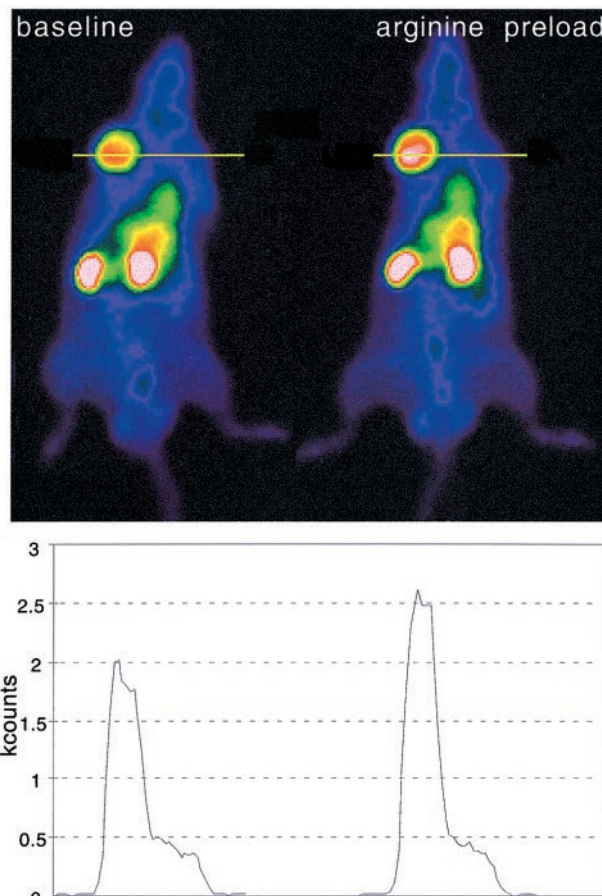


FIGURE 4. (Top) ¹²³I-3-IMT image in baseline conditions and after preload with arginine of same rat (summed data, 10–40 min after injection). (Bottom) Corresponding line profiles represent count densities along line drawn through tumor. After arginine preload, tumor uptake is increased, without increase in contralateral background region.

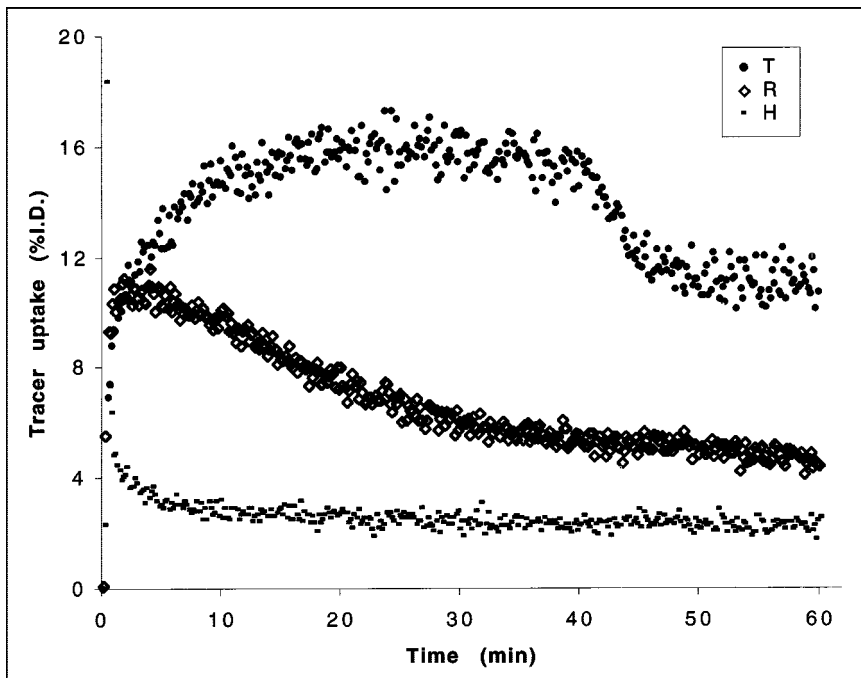


FIGURE 5. Time-activity curves of displacement study. Phenylalanine afterload was injected at 40 min. $T^{*bp, *BKG}$, tumor uptake corrected for blood-pool and background activity. $R^{*bp, *BKG}$, renal uptake corrected for blood-pool and background activity. H^{*BKG} , blood-pool activity in heart corrected for background activity.

a driving force for the uphill transport of amino acids. The resulting amino acid gradient is then used as the driving force for system L-mediated exchange of intracellularly concentrated amino acids for amino acids otherwise not transported or scarcely transported (aromatic amino acids and neutral amino acids with bulky side chains). Therefore, the exchange rate is low in cells with low intracellular

concentrations of amino acids and high in cells with high intracellular concentrations of amino acids. This effect is also called trans-stimulation of the available transporters and is distinct from adaptive regulation of the number of transporters in response to amino acid availability.

We propose that the amino acid preload in our experiments increased the intracellular amino acid pool in the tumor cells. The intracellular amino acids were then exchanged by system L for ^{123}I -3-IMT molecules, resulting in a higher rate of entry and increased total ^{123}I -3-IMT accumulation in preload conditions compared with the baseline experiments. The variable strength of the effect observed for the same molar concentration of the different amino acids in the preload can be explained by the different affinity of the preloaded amino acids for the transporter. Amino acids with a high affinity, such as tryptophan and phenylalanine, are better exchange substrates than glutamate and proline (low affinity). Arginine has a low affinity for LAT1, yet it is transported with high affinity by the y^+ LAT1 transporter subtype (16). This transporter subtype exchanges intracellular cationic amino acids (arginine, lysine) for extracellular neutral amino acids cotransported with Na^+ .

The gain in tumor contrast was reduced by an increase in background activity in all preload experiments, except for arginine. Such an increase was expected because we assume that the ubiquitous LAT1 transporter is also present in the normal cells of the background. However, the increase in the normal tissues was relatively weaker compared with the tumor tissue. We suggest that this is because the amino acid content of tumor cells is low compared with that of normal cells before the administration of the preload because of their high metabolic activity. Therefore, system L activity is stimulated more intensely in tumor cells. The absence of increase in background activity after arginine preload is possibly due to a

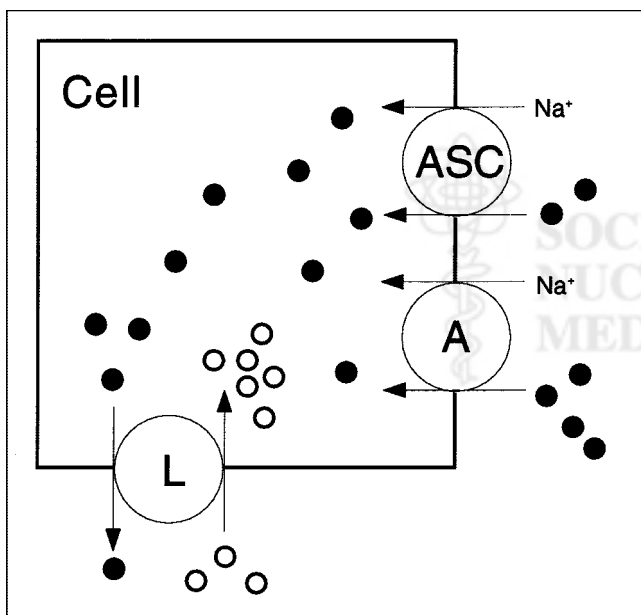


FIGURE 6. Simplified model of system L antiporter: ●, amino acids transported mainly by unidirectional systems A and ASC; ○, system L substrates. Systems A and ASC cotransport amino acids with Na^+ , using Na^+ gradient to energize transport process. System L uses amino acid gradient to energize exchange of intracellular amino acids for extracellular neutral amino acids.

different tissue expression of the γ^+ LAT1 transporter subtype: low expression in the background tissues and high expression in the tumor cells. Alternatively, it could be related to the regulatory role of arginine on system L transport: High arginine concentrations downregulate the expression of system L transporters in normal tissues, whereas a loss of response has been observed in cancer cells leading to a constitutive upregulation of system L transporter expression (17).

The displacement experiment also illustrates the exchanger mode of transporter, but now it is the intracellular ^{123}I -3-IMT that is exchanged for phenylalanine, resulting in an efflux of ^{123}I -3-IMT. Phenylalanine was used because of its good solubility and high affinity for system L.

The results are not in contradiction with the study by Langen et al. (18) that showed competition of ^{123}I -3-IMT uptake in human brain tumors during intravenous infusion of a mixture of naturally occurring L-amino acids. In their experiment a high dose of amino acids was administered before, during, and after ^{123}I -3-IMT injection. In our preload experiments we administered the amino acids only before ^{123}I -3-IMT injection. Moreover, the administered dose of amino acids was relatively low and could not induce plasma levels above the saturation level of the transport systems at the time of ^{123}I -3-IMT injection, thereby avoiding competitive effects. In theory, an optimum dose of unlabeled amino acids and according time of tracer injection exist, where there is an ideal balance between system L stimulation and competitive inhibition. In practice, we suggest that it is important to monitor the plasma concentration of the preloaded amino acid and inject the tracer when this level is sufficiently below the saturation level of the involved transport systems.

Our findings are very likely to be valid for similar PET tracers that are also predominantly accumulated by system L (L-3- ^{18}F -fluoro- α -methyltyrosine, 2- ^{18}F -fluorotyrosine, *p*- ^{18}F -fluorophenylalanine, *o*-(2- ^{18}F -fluoroethyl)-L-tyrosine, and [methyl- ^{11}C]-L-methionine) (19,20). These experiments show that the tumor uptake of ^{123}I -3-IMT is closely related to the nutritional status of the patient. The fasting state in which patients are currently studied with this type of tracer is possibly the metabolic condition in which tumor accumulation is at its lowest level. We suggest that a standardized protein-rich meal or amino acid administration before tracer injection might significantly increase tumor uptake and image contrast. However, we believe it is too early to recommend amino acid preloading for routine patient scans. Clinical studies with intraindividual comparison of tumor accumulation in sober conditions and after amino acid preload are required to prove the effect in humans and determine the best type of preload, the dose, and the time of tracer injection after preload administration.

CONCLUSION

Amino acid preload increases ^{123}I -3-IMT tumor accumulation and improves image contrast in our experiments. The

phenomenon is explained by the antiporter activity of the system L amino acid transporters. These data suggest that the fasted state might not be optimal for ^{123}I -3-IMT studies in oncologic patients. Further clinical studies are now underway to determine the optimal metabolic conditions for imaging with system L-transported tracers.

ACKNOWLEDGMENT

This work was supported by a grant from the Belgian Fonds voor Wetenschappelijk Onderzoek-Vlaanderen, Brussels, Belgium.

REFERENCES

1. Jager PL, Vaalburg W, Pruijm J, de Vries EG, Langen KJ, Piers DA. Radiolabeled amino acids: basic aspects and clinical applications in oncology. *J Nucl Med.* 2001;42:432–445.
2. Weber WA, Dick S, Reidl G, et al. Correlation between postoperative 3- ^{123}I iodo-L- α -methyltyrosine uptake and survival in patients with gliomas. *J Nucl Med.* 2001;42:1144–1150.
3. Jager PL, Franssen EJ, Kool W, et al. Feasibility of tumor imaging using L-3-[iodine-123]-iodo- α -methyl-tyrosine in extracranial tumors. *J Nucl Med.* 1998;39:1736–1743.
4. Dierickx LO, Lahoutte T, Deron P, et al. Diagnosis of recurrent head and neck squamous cell carcinoma with 3- ^{123}I iodo-L- α -methyltyrosine SPET. *Eur J Nucl Med.* 2001;28:282–287.
5. Jager PL, de Vries E, Piers DA, Timmer Bosscha H. Uptake mechanisms of L-3- ^{123}I iodo- α -methyl-tyrosine in a human small-cell lung cancer cell line: comparison with L-1- ^{14}C -tyrosine. *Nucl Med Commun.* 2001;22:87–96.
6. Lahoutte T, Cavelliers V, Dierickx L, et al. In vitro characterization of the influx of 3- ^{123}I iodo-L- α -methyltyrosine and 2- ^{123}I iodo-L-tyrosine into U266 human myeloma cells: evidence for system T transport. *Nucl Med Biol.* 2001;28:129–134.
7. Langen KJ, Bonnie R, Mühlensiepen H, et al. 3- ^{123}I iodo- α -methyl-L-tyrosine transport and 4F2 antigen expression in human glioma cells. *Nucl Med Biol.* 2001;28:5–11.
8. Franzius C, Kopka K, van Valen F, et al. Characterization of 3- ^{123}I iodo- α -methyl-L-tyrosine (^{123}I IMT) transport into human Ewing's sarcoma cells in vitro. *Nucl Med Biol.* 2001;28:123–128.
9. Verrey F, Jack DL, Paulsen IT, Saier MH, Pfeiffer R Jr. New glycoprotein associated amino acid transporters. *J Membr Biol.* 1999;172:181–192.
10. Christensen HN, Cullen AM. Intensified gradients for endogenous amino acid substrates for transport system L on injecting a specific competitor for that system. *Life Sci.* 1981;29:749–753.
11. Chavatte K, Gysemans M, Mertens J, et al. Improved synthesis and radiosynthesis of L-3-1123- α -methyltyrosine [abstract]. *Eur J Nucl Med.* 1996;23:1139.
12. Gühlke S, Biersack HJ. Simple preparation of L-3-iodo- α -methyl tyrosine suitable for use in kit preparations. *Appl Radiat Isot.* 1995;46:177–179.
13. Patlak CS, Goldstein DA, Hoffman JF. The flow of solute and solvent across a two-membrane system. *J Theor Biol.* 1963;5:426–427.
14. Peters AM. Graphical analysis of dynamic data: the Patlak-Rutland plot. *Nucl Med Commun.* 1994;15:669–672.
15. Christensen HN. Organic ion transport during seven decades: the amino acids. *Biochim Biophys Acta.* 1984;779:255–269.
16. Pfeiffer R, Rossier G, Spindler B, Meier C, Kühn L, Verrey F. Amino acid transport of type γ^+ L-type heterodimers of 4F2hc/CD98 and members of the glycoprotein associated amino acid transporter family. *EMBO J.* 1999;18:49–57.
17. Campell WA, Sah DE, Medina MM, Albina JE, Coleman WB, Thompson NL. TAI1/LAT-1/CD98 light chain and system L activity, but not 4F2/CD98 heavy chain, respond to arginine availability in rat hepatic cells: loss of response in tumor cells. *J Biol Chem.* 2000;275:5347–5354.
18. Langen KJ, Roosen N, Coenen HH, et al. Brain and brain tumor uptake of L-3- ^{123}I iodo- α -methyl tyrosine: competition with natural L-amino acids. *J Nucl Med.* 1991;32:1225–1229.
19. Heiss P, Mayer S, Herz M, Wester HJ, Schwaiger M, Senekowitsch-Schmidtke R. Investigation of transport mechanism and uptake kinetics of O-(2- ^{18}F fluoroethyl)-L-tyrosine in vitro and in vivo. *J Nucl Med.* 1999;40:1367–1373.
20. Coenen HH, Kling P, Stöcklin G. Cerebral metabolism of L-(2-[^{18}F])fluorotyrosine, a new PET tracer of protein synthesis. *J Nucl Med.* 1989;30:1367–1372.